Mineralogy and Petrology (2002) 75: 23–40

Mineralogy and Petrology

Fluorine mineralisation from burning coal spoil-heaps in the Russian Urals

E. V. Sokol, E. N. Nigmatulina, and **N. I. Volkova**

United Institute of Geology, Geophysics and Mineralogy, Russian Academy of Sciences, Novosibirsk, Russia

With 4 Figures

Received April 10, 2000;
revised version accepted February 24, 2001

Summary

Anhydrous iron, aluminum and fluorine-rich paralavas were found in the burned spoil-heaps of the Chelyabinsk coal basin, Russia. The rocks contain tridymite, anorthite, ferroan fluorine-bearing cordierite, fluorine-bearing mullite, periclase, fluorapatite, micas of the F-biotite–F-phlogopite series, fluortopaz, fluorite, and sellaite. The fluorine-rich minerals formed as a result of local thermal reactions of sedimentary carbonates and silicates with gaseous fluorine. During coal combustion fluorine concentrates in the annealed ankeritic marls where the increase of F is hundreds of times over its concentration in the initial sedimentary rocks. The formation of MgF_2 and CaF_2 promotes local melting at relatively low temperatures ($T < 1000\,^{\circ}C$) with the residuum consisting of two immiscible liquids. One crystallises as the fluorides, the other as fluorine-substituted analogues of the hydrosilicates, which under the extremely dry conditions, produce minerals containing extremely high F-contents.

Introduction

Fluorine may form independent mineral species with Na, (villiaumite, NaF), with Ca (fluorite, CaF_2), and with Mg (sellaite, MgF_2) but most usually in nature it is substituted as an additional anion in a range of mineral species characterised by the substitution $(OH)^- \rightarrow F^-$. The range of fluorine substitution varies, but as a rule, pure fluorine endmembers, are not formed. However, the complete substitution of OH^- by F^- is the basis of pyrogenic synthesis of fluorine analogues of hydrosilicates (*Putilin* et al., 1987, 1992; *Grigoryeva* et al., 1975). In the silicates without hydroxyl groups such as sphene, olivine, and garnet, fluorine can substitute for some of the oxygen, $O^{2-} + \square \rightarrow 2F^-$ (*Ekström*, 1972; *Banks*, 1976; *Kogarko* and *Krigman*, 1981; *Deer* et al., 1982; *Kleck* and *Foords*, 1999), and has also been

shown to occur among synthetic phases such as mullite (*Putilin* et al., 1987) and cordierite (*London* et al., 1999). However, the position of F as part of the silicate tetrahedra, that is the formation of Si–F bonds, is not reliably established (*Kogarko* and *Krigman*, 1981).

We investigated the extraordinarily fluorine-rich paralavas, which are the product of mutual melting of siderite rock, carbonaceous clays and mudstones caused by the burning of spoil-heaps, in the Chelyabinsk coal basin, of the South Urals, Russia. A detailed description of these spoil-heaps has been given by *Chesnokov* and *Tscherbakova* (1991), *Chesnokov* (1997, 1999), *Cesnokov* et al. (1998) and *Sokol* et al. (1998). The area contains sedimentary rocks especially mudstones, some containing siderite, and marls, which underwent spontaneous coal combustion at atmospheric pressures and temperatures ranging from 600–1300 °C. The water vapour content in this system was very low ($P_{H_2O} \ll 1$ bar). Reaction of fluorine, chlorine, and sulphur gases generated under these conditions with these sediments have resulted in any OH-bearing compounds becoming chlorine- and fluorine-substituted analogues (*Chesnokov* and *Tscherbakova*, 1991; *Chesnokov*, 1995, 1999; *Cesnokov* et al., 1998).

The main fluorine-containing minerals in these pyrometamorphic rocks are fluorite and sellaite. Fluor-silicates though not abundant are represented by minerals of the humite family, fluor-amphiboles, cuspidine–chlorocuspidine $Ca_4[Si_2O_7](F, Cl)_2$, as well as by fluorellestadite $Ca_{10}[(SO_4)_3(SiO_4)_3]F_2$. Fluorine-bearing phosphates and borates such as fluorapatite, wagnerite and fluoborite are also present. It has been suggested that these minerals are the products of gas-transport reactions (*Chesnokov* and *Tscherbakova*, 1991; *Chesnokov*, 1995, 1997; *Cesnokov* et al., 1998).

In addition to describing the mineralogy of the pyrogenic paralavas of Chelyabinsk we suggest possible mechanisms of fluorine concentration during pyrometamorphism that led to the formation of fluorine-substituted analogues of silicates and hydrosilicates.

Analytical procedure

The composition of minerals was determined by microprobe, ''Camebax-Micro'', using the general-purpose program RMA-92 (*Lavrent'ev* et al., 1991), and accelerating voltage of 20 kV, with beam current 40 nA, and beam diameter of 2–3 μm. Natural and synthetic minerals of similar composition served as standards (Table 1). Analyses were performed at a take-off angle of 40° with 10 sec counts providing the data used in the calculation of concentrations by the PAP method (*Pouchou* and *Pichoir*, 1985). Ti, Ba, Ca, and P concentrations were corrected for overlap of the $Ti_{K\alpha}$, $Ba_{L\alpha}$, $Ca_{K\beta 1}$ and $P_{K\alpha}$ peaks, with precision estimated to be better than 2% for all elements except for F for which it is about 5%. The detection limit C_{min} is calculated using 2σ-criterion (at a confidence level of 99%).

Whole-rock compositions were obtained by X-ray fluorescence analysis. H_2O and CO_2 were determined using a chromatograph LX-8 MD if the concentration was < 1.5 wt%, and by gravimetric method and titration for higher concentrations. Fluorine was analysed by photometric method with a precision of 0.003 wt%. Phase identification was made using X-ray diffractometry (DRON-3). The

Table 1. *Measurement conditions of electron microprobe analysis of minerals and glasses*

Analytical line	Crystal-analyser	Standard sample	C_{min}, detection limit, wt%
$Si_{K\alpha}$	TAP	Z-cordierite	0.009
$Ti_{K\alpha}$	PET	Glass Gl-6	0.017
$Al_{K\alpha}$	TAP	Z-cordierite	0.012
$Fe_{K\alpha}$	LiF	Garnet O-145	0.017
$Mn_{K\alpha}$	LiF	Garnet IGEM	0.014
$Mg_{K\alpha}$	TAP	Z-cordierite	0.017
$Ca_{K\alpha}$	PET	Diopside	0.015
$Na_{K\alpha}$	TAP	Albite	0.022
$K_{K\alpha}$	PET	Orthoclase Or-1	0.017
$Ba_{L\alpha}$	LiF	Glass Gl-11	0.056
$P_{K\alpha}$	TAP	F-apatite	0.006
$Cl_{K\alpha}$	PET	Cl-apatite	0.013
$F_{K\alpha}$	PC-1	F-phlogopite	0.142

transmission IR-spectra of micas were recorded using Specord 75 IR. The spectra of cordierites were determined using the IR-FOURIER spectrometer IFS-113v (''Bruker'') and incorporated diffusive reflection analysis. All the analyses were performed in the United Institute of Geology, Geophysics and Mineralogy SB RAS, Novosibirsk.

General features of fluorine-rich paralavas

The fluorine-rich paralavas were found within a high-temperature reaction zone in a gaseous blow zone near the base of a cone-shaped dump of mine 204 (Kopeisk City) and have been described as cordierite nodules (*Lotova* and *Nigmatulina*, 1989; *Chesnokov* and *Tscherbakova*, 1991; *Chesnokov* et al., 1993; *Sokol* et al., 1998). They are grey-violet, vesicular nodules, 5–20 cm in size, which are composed of fine-grained (0.5–1 mm) minerals and numerous cavities that are encrusted with a variety of crystals. The nodules are associated with black slags, the product of burning the iron-bearing carbonates, and fragments of annealed mudstone, similar to clinkers.

The textural relationships of the fluorine-containing paralavas with other rock types in the spoil-heaps and the absence of ''roots'' or inter connecting channels between the nodules, suggest that they are the products of crystallisation of small amounts of mobile local melts. *Chesnokov* et al. (1993) suggested that they may be the result of melting of argillaceous sideritic rocks under reducing conditions.

The original rocks in the Chelyabinsk coal basin are mudstones containing muscovite–illite with relic detrital quartz, and marls consisting of carbonates of the siderite–ankerite series. The chemical compositions are presented in Table 2. The bulk composition of the cordierite nodules is close to that of a mixture of sideritic marls and mudstones. The nodules differ from clinkers (partially fused metapelite rocks), and the parabasalts by high concentrations of Al_2O_3 and Fe_2O_3 (up to 20 wt%), moderate CaO and MgO contents (~ 5 wt%), very low Na_2O and water (< 0.02 wt%), and the anomalously high quantity of fluorine (up to 1.6 wt%).

Table 2. *Chemical composition of representative samples of initial and thermally altered rocks from burned spoil-heaps in the Chelyabinsk coal basin*

Component, wt%	Mudstones			Clinker	Marls		Cordierite nodules		Parabasalts	
	Initial		The first stage of annealing		Ankerite	Siderite				
	MC-1	106-1	54-37	KP-2-1	185	103-2	055E-27	055E-29	107	42-17-1
SiO_2	59.71	67.3	63.38	62.98	25.22	18.80	44.59	50.66	37.78	43.32
TiO_2	1.03	1.06	1.14	1.64	0.49	0.35	0.78	0.98	0.94	0.73
Al_2O_3	26.61	17.37	26.25	25.50	10.64	7.68	19.61	19.46	14.46	16.29
Fe_2O_3*	2.64	3.93	2.69	2.84	11.10	29.83	22.78	17.03	22.48	20.21
MnO	0.11	0.13	0.11	0.12	0.17	0.21	0.22	0.23	0.26	0.24
MgO	1.23	1.26	2.01	1.45	11.37	7.40	4.68	4.89	5.61	6.46
CaO	0.05	0.30	0.40	1.38	23.51	5.84	5.53	5.84	16.07	11.53
Na_2O	0.32	1.17	0.64	0.07	< 0.02	< 0.02	< 0.02	< 0.02	0.17	0.10
K_2O	5.73	2.02	2.00	3.11	0.31	0.71	0.85	0.35	1.46	0.77
P_2O_5	0.00	0.08	0.15	0.62	0.47	0.62	0.43	0.56	0.77	0.36
LOI	2.37	5.44	1.18	0.29	16.72	28.87	0.03	0.00	0.00	0.00
Total	99.80	100.06	99.95	100.00	100.00	100.31	99.50	100.00	100.00	100.01
H_2O	1.185	1.650	0.600	0.600	2.52	0.54	0.014	–	0.015	0.060
CO_2	0.100	–	–	–	12.12	27.50	0.002	–	0.620	0.450
F	0.079	0.030	0.003	< 0.003	0.100	0.093	1.570	0.490	0.090	0.020

* all Fe as Fe_2O_3

A detailed mineralogical study was carried out on sample 055E-27 containing 1.57 wt% of fluorine. The main mineral is ferrous cordierite (up to 50 vol%), with the following associated phases: tridymite (10–15 vol%), anorthite ($\sim$ 5–10 vol%), mullite ($<$ 5 vol%), micas of the F-phlogopite–F-biotite series ($\sim$ 3–5 vol%), and accessory minerals such as topaz, F-apatite, and periclase ($<$ 2 vol%). Opaque phases, magnetite, hematite and pseudobrookite make up 10–15 vol%. Less than 5 vol% fluorite, sellaite or K–Al acid glass were found in the intergranular space. The phases were determined by their optical characteristics, X-ray diffraction and microprobe analysis.

Mineralogical composition of the cordierite nodules

Petrographic investigations suggest that the paragenetic sequence of mineral formation in the cordierite nodules was as follows: alumospinel, plagioclase $\rightarrow$ cordierite, Al-magnetite $\rightarrow$ apatite $\rightarrow$ Ti-magnetite $\rightarrow$ Fe–Mg micas $\rightarrow$ tridymite $\rightarrow$ sellaite, fluorite, K–Al acid glass ($\pm$ hematite, pseudobrookite).

Cordierite in the nodules occurs as granular aggregates of polysynthetically twinned individuals. Prismatic pseudohexagonal crystals, frequently primitive triplets, are common in the cavities (Fig. 1). The mineral is bright violet with a clear dichroism: O ($=\gamma$) violet, E ($=\alpha$) colourless, optically negative, toward the orthorhombic modification ($\Delta = 0.29$). It is a ferroan variety (Mg# = 16–26%) of remarkable chemical composition (Table 3) with K_2O up to 0.2 wt%, an amount typical for cordierites from pyrometamorphic rocks and buchites (*Lotova* and *Nigmatulina*, 1989; *Schreyer* et al., 1990; *Sokol* et al., 1998). IR-spectroscopic

Fig. 1. Prismatic crystal of cordierite from a cavity in cordierite nodule

Table 3. *Chemical compositions of cordierites from fluoric paralavas (sample 055E-27)*

Association	Reference sample		Crd + Trd				Crd + Trd + Bt (±An; ±Mul)					
Sample	1	2	3C	3R	4C	4R	5[b]	6[b]	7	8	9C	9R[b]
SiO_2	48.89	49.00	47.12	47.33	46.56	46.39	47.04	47.10	46.49	47.03	47.01	47.18
TiO_2	0.01	0.00	0.00	0.01	0.00	0.00	0.04	0.02	0.00	0.00	0.00	0.00
Al_2O_3	33.17	33.10	32.07	32.08	32.35	32.47	31.80	31.66	32.45	32.29	32.28	32.32
FeO[a]	4.51	4.86	14.78	14.95	14.84	14.87	15.36	15.40	14.64	15.35	14.92	14.97
MnO	0.23	0.73	0.65	0.68	1.27	0.83	1.02	1.09	0.72	1.05	0.97	0.88
MgO	10.53	10.40	4.55	4.39	4.47	4.81	3.81	3.74	5.08	4.40	4.64	4.61
CaO	0.01	0.03	0.03	0.02	0.06	0.03	0.05	0.07	0.04	0.06	0.06	0.04
Na_2O	0.60	0.35	–	–	0.02	0.01	–	–	0.00	0.00	0.03	0.06
K_2O	0.22	0.05	0.00	0.00	0.05	0.09	0.04	0.10	0.05	0.02	0.06	0.05
P_2O_5	0.11	–	0.01	0.00	–	–	0.00	0.01	–	–	–	–
BaO	–	–	0.02	0.01	–	–	0.00	0.00	–	–	–	–
Cl	–	–	0.01	0.00	0.01	0.02	0.01	0.01	0.02	0.01	0.00	0.02
F	0.22	0.08	0.10	0.16	0.17	0.22	0.30	0.22	0.17	0.22	0.19	0.18
Total	98.50	98.60	99.35	99.64	99.80	99.74	99.47	99.41	99.66	100.43	100.16	100.31
$O–(F_2)$	0.09	0.03	0.05	0.07	0.07	0.09	0.12	0.09	0.07	0.09	0.08	0.08
Total	98.63	98.57	99.30	99.57	99.73	99.65	99.35	99.32	99.59	100.34	100.08	100.23
Mg#	68.96	76.80	34.43	33.35	33.07	35.30	29.29	28.77	37.07	32.33	34.21	34.13
Si	4.98	5.20	4.96	4.97	4.91	4.88	4.97	4.98	4.89	4.93	4.93	4.94
Ti	0.00	0.00	0.00	0.00	0.00	0.00	0.00	0.00	0.00	0.00	0.00	0.00
Al	3.98	4.14	3.98	3.97	4.02	4.03	3.96	3.95	4.02	3.99	3.99	3.98
Fe	0.38	0.43	1.30	1.31	1.31	1.31	1.36	1.36	1.29	1.34	1.31	1.31
Mn	0.02	0.07	0.06	0.06	0.11	0.07	0.09	0.10	0.06	0.09	0.09	0.08
Mg	1.60	1.65	0.71	0.69	0.70	0.75	0.60	0.59	0.80	0.69	0.72	0.72
Ca	0.00	0.00	0.00	0.00	0.01	0.00	0.01	0.01	0.00	0.01	0.01	0.00
K	0.03	0.07	0.00	0.00	0.01	0.01	0.01	0.01	0.01	0.00	0.01	0.01
P	0.01	0.01	0.00	0.00	–	–	0.00	0.00	–	–	–	–
Ba	–	–	0.00	0.00	–	–	0.00	0.00	–	–	–	–
F	0.07	0.02	0.03	0.05	0.06	0.07	0.10	0.07	0.06	0.07	0.06	0.06
Grain size, μm			30	30	200	200	20	50	40	50	50	50

(*continued*)

Table 3 (*continued*)

Association	Crd + Trd + Bt + F-ap	Crd + Trd + Toz(±An; ±Mul)							Crd + Trd + Fl (±An; ±Mul)		Crd + Trd + MgF_2 + Fl(±An)		
Sample	10	11	12 C	12 R[b]	13	14 C	14 R[b]	15	17	18[b]	19	20 C	20 R[b]
SiO_2	47.86	48.08	48.15	47.65	48.78	48.93	48.79	48.06	46.43	47.31	47.67	46.25	46.11
TiO_2	0.00	0.02	0.02	0.01	0.03	0.03	0.02	0.00	0.01	0.01	0.01	0.00	0.00
Al_2O_3	32.09	31.69	31.79	31.93	32.02	31.46	31.26	32.41	32.55	31.62	32.12	31.63	31.46
FeO[a]	14.57	14.49	13.65	14.75	13.98	13.66	14.06	13.79	14.95	14.97	13.89	16.10	16.76
MnO	0.71	1.46	0.68	1.27	0.92	0.76	0.95	0.75	0.89	0.68	1.10	1.04	1.22
MgO	4.36	3.71	4.99	3.62	4.60	4.76	4.27	4.74	4.66	5.47	4.09	4.06	3.33
CaO	0.03	0.07	0.04	0.09	0.02	0.03	0.04	0.06	0.11	0.01	0.19	0.08	0.14
Na_2O	–	–	–	–	–	–	–	–	0.04	0.00	–	0.00	0.00
K_2O	0.03	0.14	0.05	0.19	0.05	0.03	0.07	0.07	0.06	0.04	0.10	0.07	0.35
P_2O_5	0.01	0.02	0.00	0.00	0.00	0.00	0.00	0.00	–	–	0.00	–	–
BaO	0.03	0.00	0.00	0.00	0.00	0.00	0.05	0.00	–	–	0.00	–	–
Cl	0.01	0.02	0.01	0.01	0.01	0.02	0.01	0.01	0.00	0.00	0.01	0.01	0.01
F	0.07	0.15	0.25	0.25	0.15	0.24	0.39	0.18	0.27	0.15	0.20	0.19	0.28
Total	99.77	99.84	99.62	99.77	100.55	99.92	99.90	100.06	99.97	100.26	99.38	99.43	99.66
O–(F_2)	0.03	0.07	0.10	0.11	0.06	0.11	0.16	0.07	0.09	0.06	0.08	0.08	0.12
Total	99.74	99.77	99.52	99.66	100.49	99.81	99.74	99.99	99.86	100.20	99.30	99.35	99.54
Mg#	33.70	29.28	38.28	28.69	35.48	37.03	33.63	36.74	34.38	38.37	32.70	29.67	24.80
Si	5.01	5.04	5.03	5.01	5.05	5.09	5.09	5.00	4.88	4.95	5.01	4.92	4.92
Ti	0.00	0.00	0.00	0.00	0.00	0.00	0.00	0.00	0.00	0.00	0.00	0.00	0.00
Al	3.96	3.92	3.91	3.96	3.91	3.86	3.84	3.97	4.03	3.90	3.98	3.96	3.96
Fe	1.28	1.27	1.19	1.30	1.21	1.19	1.23	1.20	1.31	1.31	1.22	1.43	1.50
Mn	0.06	0.13	0.06	0.11	0.08	0.07	0.08	0.07	0.08	0.06	0.10	0.09	0.11
Mg	0.68	0.58	0.78	0.57	0.71	0.74	0.66	0.73	0.73	0.85	0.64	0.64	0.53
Ca	0.00	0.01	0.00	0.01	0.00	0.00	0.00	0.01	0.01	0.00	0.02	0.01	0.02
K	0.00	0.02	0.01	0.03	0.01	0.00	0.01	0.01	0.01	0.01	0.01	0.01	0.05
P	0.00	0.00	0.00	0.00	0.00	0.00	0.00	0.00	–	–	0.00	–	–
Ba	0.00	0.00	0.00	0.00	0.00	0.00	0.00	0.00	–	–	0.00	–	–
F	0.02	0.05	0.08	0.08	0.05	0.08	0.13	0.06	0.09	0.05	0.07	0.06	0.09
Grain size, μm	40	30	60	60	20	20	20	40	40	10	30	25	25

Note: *1* synthetic fluorine-bearing cordierite (*London* et al., 1999); *2* standard Z-cordierite sample (mean of the 15 analyses). *Mg#* $Mg/(Mg + Fe + Mn) \cdot 100\%$. [a] All Fe as FeO. Cordierite formula was calculated on the basis of 18 cations. *An* anortite; *Ap* apatite; *Bt* biotite; *Crd* cordierite; *Trd* tridymite; *Toz* topaz; *Fl* fluorite; *Mul* mullite. [b] cordierites which are in the immediate contact (5–10 μm) with fluorine-bearing phases. -: not determined

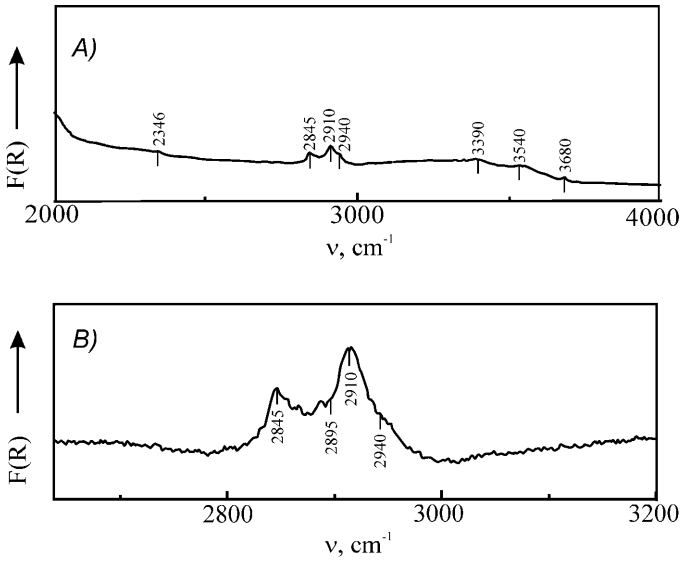

Fig. 2. General IR-spectrum of diffusive reflection of cordierite (sample 055E-27) **A** characteristic bands of fluid components $-H_2O$ (3500–3700 cm^{-1}), CO_2 (2235–2500 cm^{-1}) and C_nH_m (2800–3200 cm^{-1}); **B** bands of valent CH-vibrations

examination showed a lack of CO_2 and trace quantities of water (Fig. 2). The spectrum bands $\nu = 2845$; 2910; 2940 cm^{-1}, correspond to vibrations of CH_3-groups (*Lepezin* et al., 1999).

In order to estimate qualitatively the influence of fluorine activity on cordierite composition we have analysed cordierite crystals immediately adjacent to tridymite and anorthite, as well as from the association with various fluorine-bearing minerals; i.e. topaz, fluorapatite, F-biotite, fluorite and sellaite (see Table 3). The accuracy of the results was verified by parallel analyses of fluorine concentrations in the natural reference Z-cordierite sample (see Table 1) and in tridymite from the analysed sample (Table 4). It was established that the mean fluorine content (of 15 analyses) in the Z-cordierite reference sample was 0.08 wt%, that is less than the lower limit of detection (0.14 wt%) for this element. Fluorine in tridymite was not found.

Cordierite associated with tridymite and anorthite contains 0.10–0.22 wt% of F. The concentration of fluorine in cordierite coexisting with fluorine-bearing minerals is slightly higher and reaches a maximum of 0.39 wt% when it is in contact with topaz. The increased contents of fluorine are characteristic not only for rims, but also for cores of cordierite crystals (0.19–0.25 wt%). We emphasise that there are no microinclusions of fluorides in the analysed cordierite grains. The preliminary results of IR- and Raman-spectroscopic investigations do not allow to pin down the structural position of fluorine unambiguously.

Micas of the biotite–phlogopite series form laths in the groundmass, as well as thin sectorial plates in the cavities were analysed. Mg# varies from 38 up to 64% while the BaO content may reach 2 wt%. These fluor-micas with up to 7.29 wt% represent the F-richest natural Mg–Fe micas reported to date (*Nash*, 1993; *Stoppa*

Table 4. *Representative chemical compositions of minerals and glasses from fluoric paralavas (sample 055E-27)*

Sample	Mica				Anorthite		Tridymite					Topaz						Apatite	Periclase		Glass	
	1	2	3	4	5	6	7	8	9	$X_{mean.}$	S_r	10	11	12	13	$X_{mean.}$	S_r	14	15	16	17	18
										$n=22$							$n=8$						
SiO_2	42.90	40.23	36.99	39.08	44.56	44.41	98.41	98.92	99.03	*99.03*	*0.41*	33.34	31.42	30.60	31.90	*31.39*	*0.46*	0.62	0.60	0.04	73.72	72.98
TiO_2	–	0.25	0.85	0.99	0.03	0.00	0.07	0.11	0.13	*0.08*	*0.02*	–	0.17	0.14	0.07	*0.14*	*0.05*	0.00	0.00	0.00	0.06	0.07
Al_2O_3	13.03	14.78	14.96	16.05	35.07	35.20	0.26	0.27	0.12	*0.16*	*0.04*	50.96	55.26	55.48	55.46	*55.39*	*0.10*	0.00	0.00	0.05	13.37	13.33
FeO*	0.06	10.67	20.10	12.13	0.60	0.70	0.34	0.29	0.14	*0.21*	*0.08*	0.33	0.49	0.31	0.69	*0.53*	*0.18*	1.53	0.85	0.87	0.46	0.83
MnO	–	0.26	0.59	0.77	0.08	0.10	0.01	0.02	0.02	*0.01*	*0.01*	–	0.04	0.02	0.02	*0.02*	*0.01*	0.72	0.16	0.20	0.03	0.06
MgO	29.03	18.29	11.88	16.48	0.03	0.04	0.00	0.00	0.00	*0.00*	*0.00*	0.63	0.07	0.17	0.06	*0.09*	*0.04*	0.19	95.60	97.80	0.04	0.79
CaO	–	0.04	0.00	0.01	19.53	19.34	0.02	0.01	0.02	*0.04*	*0.06*	1.82	0.11	0.10	0.00	*0.11*	*0.11*	53.92	2.44	0.66	0.92	0.43
Na_2O	0.15	0.02	0.04	0.05	0.08	0.03	0.00	0.00	0.00	*0.00*	*0.00*	–	–	–	–	–	–	–	0.09	0.08	0.06	0.05
K_2O	9.58	9.60	8.75	9.72	0.20	0.13	0.25	0.27	0.15	*0.17*	*0.04*	–	0.05	0.02	0.01	*0.04*	*0.04*	0.07	0.00	0.00	7.87	7.75
P_2O_5	–	0.10	0.01	0.02	0.04	0.05	0.00	0.00	0.00	*0.00*	*0.00*	–	1.01	1.61	0.30	*0.87*	*0.50*	41.62	–	–	0.37	0.92
BaO	–	1.58	1.70	0.76	–	–	–	–	–	–	–	–	0.04	0.01	0.00	*0.02*	*0.02*	0.00	–	–	0.06	0.07
Cl	–	0.01	0.02	0.02	–	–	0.00	0.00	0.00	0.00	0.00	–	0.01	0.01	0.00	*0.01*	*0.01*	0.01	–	–	0.03	0.03
F	8.40	7.06	7.10	7.29	–	–	0.00	0.00	0.00	0.00	0.00	19.2	19.39	19.36	19.24	*19.26*	*0.13*	2.28	–	–	0.55	0.61
Total	103.15	102.89	102.99	103.36	100.22	100.00	99.35	99.89	99.61	*99.72*	*0.43*	106.28	108.04	107.84	107.75			100.95	99.74	99.70	97.54	97.92
O–(F_2)	3.54	2.97	2.98	3.06			0.00	0.00	0.00			8.06	8.14	8.13	8.08			0.96			0.23	0.26
Total	99.61	99.93	100.01	100.30			99.35	99.89	99.61			98.22	99.90	99.70	99.67	99.79	0.28	99.99			97.31	97.66
Mg#	99.76	62.59	36.48	56.09																		
	O = 24				O = 8		O = 2					O = 6						O = 26	O = 1			
Si	6.00	5.98	5.76	5.81	2.06	2.06	0.99	0.99	1.00	*1.00*	*0.001*	1.05	0.97	0.95	0.99	*0.97*	*0.016*	0.11	0.00	0.00		
Ti	–	0.03	0.10	0.11	0.00	0.00	0.00	0.00	0.00	*0.00*	*0.000*	–	0.00	0.00	0.00	*0.00*	*0.001*	0.00	0.00	0.00		
Al	2.15	2.59	2.74	2.81	1.91	1.92	0.00	0.00	0.00	*0.00*	*0.000*	1.89	2.01	2.02	2.02	*2.02*	*0.007*	0.00	0.00	0.00		
Fe	0.01	1.33	2.62	1.51	0.02	0.03	0.00	0.00	0.00	*0.00*	*0.000*	0.01	0.01	0.01	0.02	*0.01*	*0.005*	0.22	0.00	0.00		
Mn	–	0.03	0.08	0.10	0.00	0.00	0.00	0.00	0.00	*0.00*	*0.000*	–	0.00	0.00	0.00	*0.00*	*0.000*	0.10	0.00	0.00		
Mg	6.05	4.05	2.76	3.65	0.00	0.00	0.00	0.00	0.00	*0.00*	*0.000*	0.03	0.00	0.01	0.00	*0.00*	*0.002*	0.05	0.97	0.99		
Ca	–	0.01	0.00	0.00	0.97	0.96	0.00	0.00	0.00	*0.00*	*0.001*	0.06	0.00	0.00	0.00	*0.00*	*0.004*	9.82	0.02	0.00		
K	1.71	1.82	1.74	1.84	0.01	0.01	0.00	0.00	0.00	*0.00*	*0.001*	–	0.00	0.00	0.00	*0.00*	*0.002*	0.01	0.00	0.00		
P	–	0.01	0.00	0.00	0.00	0.00	0.00	0.00	0.00	*0.00*	*0.000*	–	0.03	0.04	0.01	*0.02*	*0.013*	5.99	–	–		
Ba	–	0.09	0.10	0.04	–	–	–	–	–	–	–	–	0.00	0.00	0.00	*0.00*	*0.000*	0.00	–	–		
F	3.71	3.32	3.49	3.43	–	–				*0.00*	*0.000*	1.91	1.89	1.89	1.88	*1.88*	*0.010*	1.23	–	–		

Note: *1* synthetic fluorphlogopite (*Putilin* et al., 1987); *2–9* minerals from cordierite nodules; *10* topaz from ongonites (*Kovalenko* and *Kovalenko*, 1976); *11–18* minerals and glasses from cordierite nodules. *Mg#* $Mg/(Mg+Fe+Mn)\cdot 100\%$. * All Fe as FeO. -: not determined

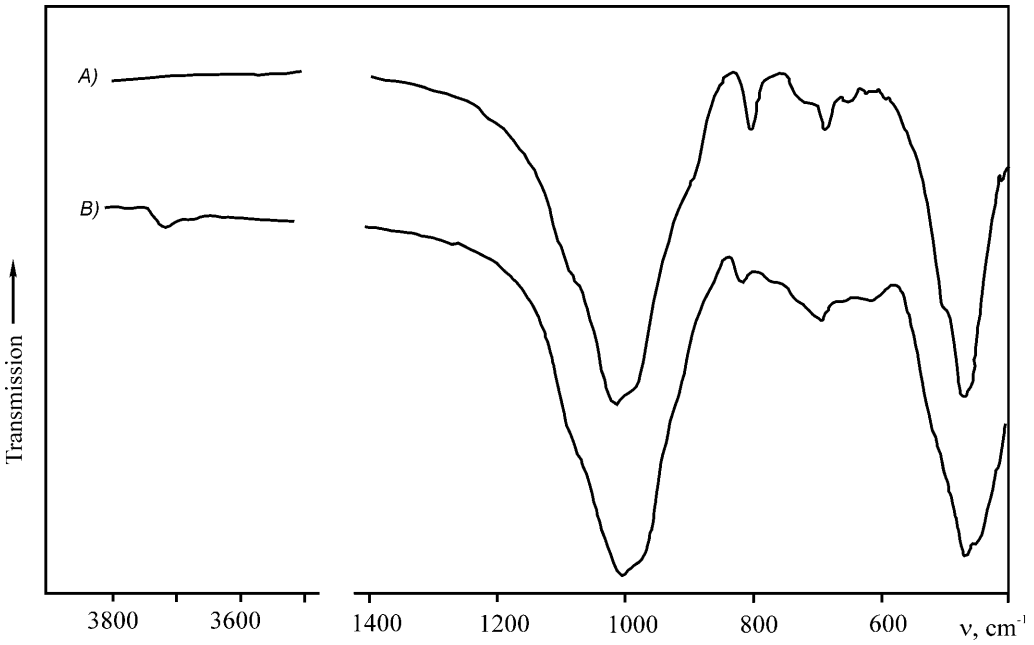

Fig. 3. General IR-spectrum of fluorphlogopite (sample 055E-27). A) in comparison with spectrum of natural hydroxil-bearing phlogopite. B) The field of OH-vibrations ($\nu = 3650$–$3710\,cm^{-1}$)

et al., 1996; *Pesquera* et al., 1999) and approximate fully substituted F-biotite and phlogopite, respectively. The IR-spectrum confirms the lack of $(OH)^-$-groups in these minerals (Fig. 3).

Plagioclase is represented by polysynthetically-twinned individuals. In the cavities, it occurs as crystals flattened along (010). The mineral is close to pure anorthite ($Na_2O < 0.1$ wt%) and is characterised by an FeO content up to 0.7 wt%, excess Si and deficient Al, compared with stoichiometric $CaAl_2Si_2O_8$.

Tridymite occurs as thin plates in the groundmass and as aggregates of hexagonal tabular crystals and sectorial twins in the cavities. Based on optical and X-ray diffraction characteristics it is the monoclinic modification. Among all polymorphs of SiO_2, tridimyte is characterised by the ability to concentrate impurities. This fact was already noted for tridymite from coal-fire buchites from Wyoming, USA (*Cosca* et al., 1989). In these tridymites the FeO is up to 0.8 wt%, Al_2O_3 up to 0.3 wt%, TiO_2 up to 0.2 wt% and K_2O up to 0.3 wt%. Fluorine was not detected.

Mullite is present in two morphologies. In the matrix of the rock it occurs as colourless needles of extremely small size (approximately $1 \times 20\,\mu m$) which were not suitable for microprobing. The presence of this phase was determined by X-ray diffraction. Coarse (0.5 mm) acicular yellow needles and obelisk-shaped crystals up to a length of 3 mm are common in the cavities (Fig. 4). Only the obelisk-shaped crystals of mullite were analysed (Table 5). They are associated with anorthite, cordierite, infrequently with magnetite or fluor-micas and are not in immediate contact with tridymite. In this case the calculated x value, reflecting a deficit in the oxygen partial lattice (*Burnham*, 1964; *Cameron*, 1977), is close to 0.32, i.e. it

Fig. 4. Cavity in cordierite nodule, encrusted by obelisk-shaped crystals of mullite

Table 5. *Chemical compositions of mullites from fluoric paralavas (sample 055E-27)*

Sample	1	2	3	4
SiO_2	27.55	25.03	25.07	25.05
TiO_2	–	0.31	0.24	0.28
Al_2O_3	70.60	68.95	68.85	68.97
Fe_2O_3	0.08	5.76	5.34	5.48
MnO	–	0.01	0.00	0.01
MgO	–	0.18	0.15	0.12
F	1.19	0.31	0.61	0.66
Total	99.42	100.55	100.26	100.57
$O–(F_2)$	0.50	0.13	0.26	0.28
Total	98.92	100.42	100.01	100.29
Si	1.48	1.35	1.35	1.35
Ti	–	0.01	0.01	0.01
Al	4.49	4.37	4.38	4.38
Fe	0.00	0.26	0.24	0.25
Mn	–	0.00	0.00	0.00
Mg	–	0.01	0.01	0.01
F	0.20	0.05	0.10	0.11
Al + Fe	4.49	4.63	4.62	4.63
Si + Al + Fe	5.97	5.97	5.98	5.98
x = (2-Si)/2	0.26	0.33	0.32	0.32

Note: *1* synthetic fluorine-bearing mullite (*Putilin* et al., 1987); *2–4* mullites from cordierite nodules. -: not determined

essentially exceeds a value of 0.25, which is characteristic for mullite $3Al_2O_3 \cdot 2SiO_2$ from SiO_2-rich associations (*Deer* et al., 1982). The studied mullite contains up to 5.76 wt% of Fe_2O_3 and up to 0.7 wt% of F. These results are corroborated by experimental studies; e.g. fluorine-bearing mullites containing up to 1.2 wt% of F were synthesised by *Putilin* et al. (1987).

Topaz and *fluorapatite* occur as single idiomorphic grains. The content of fluorine in topaz (19 wt%) is close to the maximum. The age relation with other phases is not clear. Apatite is most likely an oxyfluorapatite and is enriched in Si, Fe, and Mn.

Fluorite and *sellaite* are the last phases to crystallise. They are predominantly present in the intergranular spaces and are xenomorphic. Sometimes they form drop-shaped inclusions within biotite laths. The mineral compositions are close to the theoretical ones (Table 6).

Glass is uncommon and occurs only in the interstices. Its composition is very similar to K–Al acid residual glasses already described in parabasalts (*Sharygin* et al., 1999) with a fluorine content < 0.6 wt%.

Table 6. *Chemical compositions of fluorite and sellaite from fluoric paralavas (sample 055E-27)*

Component,	Fluorite			Component,	Sellaite	
wt%	1	2	3	wt%	4	5
Ca	51.64	51.41	51.19	Mg	38.23	38.18
F	47.33	47.37	47.28	F	60.56	60.39
Cl	0.01	0.02	0.00	Cl	0.01	0.01
P_2O_5	0.00	0.00	0.00	P_2O_5	0.00	0.00
K_2O	0.01	0.00	0.01	K_2O	0.03	0.00
Na_2O	0.11	0.13	0.16	Na_2O	0.00	0.10
MgO	0.30	0.29	0.36	CaO	0.45	0.44
MnO	0.11	0.11	0.12	MnO	0.12	0.15
FeO	0.13	0.21	0.42	FeO	0.56	0.75
Al_2O_3	0.00	0.00	0.00	Al_2O_3	0.00	0.00
TiO_2	0.00	0.00	0.00	TiO_2	0.05	0.00
SiO_2	0.05	0.05	0.12	SiO_2	0.03	0.12
Total	99.68	99.60	99.66	Total	100.04	100.14
Si	0.00	0.00	0.00	Si	0.00	0.00
Ti	0.00	0.00	0.00	Ti	0.00	0.00
Al	0.00	0.00	0.00	Al	0.00	0.00
Fe	0.00	0.00	0.00	Fe	0.00	0.01
Mn	0.00	0.00	0.00	Mn	0.00	0.00
Mg	0.01	0.01	0.01	Mg	0.99	0.99
Ca	1.01	1.01	1.00	Ca	0.00	0.00
Na	0.00	0.00	0.00	Na	0.00	0.00
K	0.00	0.00	0.00	K	0.00	0.00
P	0.00	0.00	0.00	P	0.00	0.00
Total	1.02	1.02	1.02	Total	1.00	1.00
Cl	0.00	0.00	0.00	Cl	0.00	0.00
F	1.96	1.96	1.96	F	2.00	2.00

Opaque minerals are customary phases in this association. During the crystallisation of the fluorine-rich paralavas the first mineral to form was Al-magnetite, followed by Ti-magnetite, pseudobrookite and finally hematite. Crystals of these minerals are usually found as incrustations in the cavities.

Formation conditions of fluorine-rich paralavas

The mechanism of fluorine concentration

Chesnokov (1997, 1999) has noted that during combustion of spoil-heap rocks the heat and mass transfer proceeds mainly by gas convection. As the thermal transformation process intensifies, the heat source migrates deeper into the spoil-heaps involving new blocks of sedimentary rocks, which provide a stable gas flow on degassing. The combustion of large spoil-heaps results in mixtures juxtaposing a variety of different mineral associations.

Striking examples of these phenomena are high-temperature associations in the metacarbonate rocks. Their formation proceeds in two stages. In the first stage in the temperature range of 600 to 1000 °C decarbonation reactions $MeCO_3 \rightarrow MeO + CO_2$ took place. At T = 700–750 °C dolomite dissociates with the formation of a powdered periclase (MgO) and calcite. At higher temperature calcite decomposes to yield a powdered lime (CaO). Siderite is characterised by the lowest temperature of decomposition, its dissociation begins already at 600 °C. Composition of the ultimate annealing products of ankerite and siderite rocks is governed by both oxygen fugacity, and concentrations of calcium and magnesium in the system. During annealing under reducing conditions fragments of siderite rocks are replaced by porous aggregates of pyrrhotite, magnetite, and wustite (FeO). Periclase, cohenite (Fe_3C), sellaite (MgF_2), fluorite, graphite can be associated with these minerals. Similar associations are preserved only in the inner parts of the burned spoil-heaps, which are protected from any contact with atmospheric oxygen and moisture. Under moderate reducing conditions (oxygen fugacity is close to the FeO–$FeFe_2O_4$ buffer), siderite decomposes according to the reaction $FeCO_3 \rightarrow FeO + FeFe_2O_4 + CO_2 + CO$. In this case wustite is not preserved and usually oxidised to magnetite and hematite. The latter minerals also originate by reaction of siderite under oxidising conditions (*Chesnokov* and *Tscherbakova,* 1991; *Chesnokov,* 1997). The ankerite annealing products have the most complicated composition. Along with lime, periclase and ferropericlase, admixtures of ferrospinellides of the magnetite–magnesioferrite series occur frequently, as well as various calcium ferrites – $Ca_2Fe_2O_5$ (srebrodolskite), $CaFe_2O_4$ and $CaFe_4O_7$ (*Chesnokov* and *Tscherbakova,* 1991; *Chesnokov,* 1997; *Sokol* et al., 2000).

The second stage commences when the metacarbonate material interacts with hot gas jets. Lime (CaO) is an effective precipitant of a wide spectrum of anions– S^{2-}, $(SO_4)^{2-}$, Cl^-, F^-, while periclase is a precipitant of fluorine only.

Cesnokov et al. (1998) investigated the high-temperature (T = 1000–1200 °C) mineral associations that originated from interaction of decarbonatised sedimentary materials with gaseous compounds of sulphur. Under reducing conditions the common product of these reactions is oldhamite CaS, and under oxidising conditions the reaction products are anhydrite and fluorellestadite. In the presence of chlorine, $CaCl_2$ and calcium chloride–silicates are formed. The rather low

concentrations of chlorine and sulphur away from the immediate heat source means that the formation of minerals with high concentrations of these elements occur only in the local zones of gaseous discharge.

The fluorine-containing paralavas present a new type of rock-gas interaction product: i.e. dehydrated and decarbonatised sedimentary material reacting with a variety of hot gases.

The main sources of fluorine are the mudstones in which fluorine is a constituent of the micas and the siderite concretions (the enclosed fluorine-bearing phosphates) (see Table 2). During combustion these minerals decompose and fluorine is transported as gas, presumably, in the form of the volatile fluorides SiF_4, AlF_3, NaF. In addition to escaping into the atmosphere fluorine is redistributed within the spoil-heap. The fluorine contents decreased by one order of magnitude in the clinker, but increased by two orders in metacarbonate segregations in comparison with the initial rocks.

The reaction of CaO and MgO with fluorine-bearing gases gives rise to fluorite and sellaite. The appearance of fluorides of K, Na and Ba is also possible. All these compounds are low-melting phases relative to silicate and oxide components: BaF_2–MgF_2 ($T_{eutectic} = 912\,^{\circ}C$); KF–$AlF_3$ ($T_{eutectic} = 580\,^{\circ}C$); MgF_2–CaF_2 ($T_{eutectic} = 945\,^{\circ}C$) (*Putilin* et al., 1987). The increased fluorine content therefore favours the formation of rather low-temperature ($T \leq 1000\,^{\circ}C$) melts that incorporate all the constituents of the sedimentary substratum in the melting process.

Peculiarities of the crystallisation processes of fluor-silicate melts

In natural silicate melts, fluorine behaviour is mainly governed by crystal fractionation (*Edgar* et al., 1996). It does not enter into the composition of main rock-forming minerals and therefore accumulates in the residual liquids. Fluorine does, however, have an influence upon mineral equilibria even when its content is less than 1 wt%. At 2–4 wt% fluorine contributes to liquid immiscibility with the formation of two compositionally different melts – one in which the cations Na, Ca, and Mg are associated with the fluorine, and a normal silicate melt (*Kogarko* and *Krigman*, 1981). The immiscibility phenomena in synthetic fluor-silicate systems are well documented (*Takusagawa* and *Saito,* 1972; *Grigoryeva* et al., 1975; *Putilin* et al., 1987). The existence of neutral fluoride complexes in diopside–fluoride melts has also been noted (*Dingwell,* 1989).

One of the consequences of the presence of fluorine in silicate melts is the expansion of the crystallisation fields of the SiO_2 polymorphs (*Kogarko* and *Krigman,* 1981). The separation of a fluorine-cation liquid promotes silicification of the coexistent second melt. The increased SiO_2 activity in melts in the presence of fluorine was noted for the systems $KAlSiO_4$–Mg_2SiO_4–SiO_2 (*Foley* et al., 1986a), CaO–CaF_2–SiO_2 (*Luth*, 1988a), $NaAlSiO_4$–$CaMgSi_2O_6$–SiO_2 (*Luth*, 1988b) and for natural ultrapotassic rocks (*Foley* et al., 1986b).

Crystallisation of fluorine-containing paralavas

The paragenetic sequence and the chemical composition of the minerals in fluorine-containing paralavas can be explained by fractionation and accumulation

of fluorine during the crystallisation of the melt. The first formed minerals are Al-Mg-spinel, anorthite and Al-magnetite followed by cordierite. Cordierite crystallisation changes the proportions of residual liquid components in favour of K, Ba, P and F, thus favouring the crystallisation of F-micas and F-apatite. After 70% of the melt crystallised (the rock contains spinel + anorthite + magnetite + cordierite) the fluorine content in the melt is estimated to be more than 3.5 wt%, a concentration that gives rise to the immiscible silicate and fluoride liquids.

These liquids evolve as a heterogeneous system. One liquid has high Ca, Mg and F concentrations, the other contains increased contents of K, Al and Si. The crystallisation path is confirmed by the appearance of rounded segregations of the fluorides CaF_2 and MgF_2 at the periphery of fluorbiotite laths, and the concurrent crystallisation of tridymite. The last crystallising phases, fluorite and sellaite, are also associated with a K–Al acid glass, the product of quenching the silicate melt; although this is rarely observed.

Mullite formation presents an interesting problem. Microcrystalline mullite, most likely a product of dehydroxylation reactions of layered silicates (*Gualtieri* et al., 1995), probably originates during the annealing of the marl, and is maintained as a residual component at all temperature ranges of nodule formation. Crystals of fluorine-bearing mullite, which occur only in cavities, are the products of synthesis in a gaseous environment.

The minerals crystallised in the nodule cavities formed, in our opinion, through mechanisms of gas-transport exchange reactions similar to those described in pyrogenic synthesis (*Putilin* et al., 1987, 1992). The order of formation of these minerals reconstructed from their relationships is as follows: tridymite, anorthite, Fe-spinels → mullite → cordierite → F-mica, occasionally hematite, pseudobrookite and α-cristobalite terminate the crystallisation process.

Fluorine-bearing silicates

The most unusual fluorine-bearing silicates observed in this study are cordierite and mullite. Only the partitioning of F^- and Cl^- into the structure of the natural anhydrous silicate, sphene, has been studied in detail (*Ekström,* 1972; *Deer* et al., 1982). In this mineral the oxygen atoms coordinated with Ca^{2+} could be substituted by F^-, Cl^- or $(OH)^-$ and the fluorine content in sphene ranges between 0.5 and 1.9 wt%. The synthesis of mullites with high concentrations of fluorine (1–1.2 wt%) has been demonstrated by *Putilin* et al. (1987). It has been suggested that one of the oxygen atoms which is coordinated with Al^{3+} may be substituted by F^- or $(OH)^-$.

Thus, in the structures of anhydrous silicates, fluorine substitutes for oxygen but not for O in the (SiO_4)–tetrahedra. This circumstance is consistent with notions by *Kogarko* and *Krigman* (1981) that silicon will neither form stable complexes with fluorine in melts, nor in polyatomic minerals. In this context the detection of fluorine in cordierite, a framework alumosilicate, is particularly remarkable. Cordierite containing 0.2–0.3 wt% of F has been synthesised in a system simulating phosphorus-bearing peraluminous granites with fluorine concentrations of 0.3–0.5 wt%. (*London* et al., 1999), although this fact remained without explanation. Our own spectroscopic investigations aiming to understand the possible structural position of

fluorine in the cordierite structure has not yet provided the appropriate information to answer this question.

Conclusions

A new type of ferrous and aluminous paralavas with fluorine contents of up to 1.6 wt% has been found in burned spoil-heaps of the Chelyabinsk coal basin. The following minerals occurring in nodules at this site have chemical compositions heretofore unreported in nature: micas, topaz, cordierite, and mullite. The formation of rocks containing such aberrant minerals is considered to be a multistage process.

During *the initial stage* heating of the spoil-heap to temperatures $\leq$650 °C, the following reactions occured: a) Thermal destruction of any layered silicates, b) Release of water and fluorine gases a portion of which is boiled off and escapes from the spoil-heap, c) Decomposition of local carbonate rock with outgassing of CO_2 and the formation of aggregates composed of lime, periclase, as well as Ca and Mg ferrites.

At *a later stage* the inner parts of the spoil-heap reach 1000–1200 °C and the combustion spreads out deeper involving blocks of previously unaltered sedimentary rocks, which continue to supply fluorine to hot gas jets. Lime and periclase act as precipitants. By this means local sites can become enriched in fluorine by factors of several hundred compared to the initial sediments. The reactions between CaO, MgO and fluorine result in the synthesis of fluorite and sellaite, which are classic fluxes used in pyrosynthethic systems. These minerals stimulate melting in the burning spoil-heaps at rather low temperatures ($T \leq 1000$ °C). The processes of melting are restricted to sites where there is annealed marl.

On *cooling* of the spoil-heap, fluorine–silicate melts crystallise, with fluorine accumulating in the residual liquid. Under these lower temperature and low water conditions, topaz, fluorbiotite and fluorapatite crystallise. Fluorine is incorporated into the structures of mullite and cordierite substituting for oxygen possibly following the scheme alumosilicate $+ 2\ F^- \rightarrow$ fluor-alumosilicate $+ O^{2-}$.

Acknowledgements

We thank *B. V. Chesnokov* for long-term fruitful cooperation, for the collection of cordierite nodules, as well as for his help with organisation of field work in the region of the Chelyabinsk coal basin. The authors have benefited greatly from the comments by *H. C. W. Skinner* (Yale University, USA) which helped to improve the original manuscript. We wish to thank *G. G. Lepezin, V. V. Sharygin, V. G. Tomas* and *V. M. Kalugin* for critical comments and scientific discussion. The helpful comments of an anonymous reviewer and Assistant Editor *J. G. Raith* are gratefully acknowledged. Financial support was given by the Russian Fund for Fundamental Research (N 98-05-65257).

References

Banks NG (1976) Halogen contents of igneous minerals as indicators of magmatic evolution of rocks associated with the Ray porphyry copper deposit, Arizona. J Res US Geol Sur 4: 91–117

Burnham CW (1964) Crystal structure of mullite. Carnegie Inst Wash Year Book 63: 223–227

Cameron WE (1977) Mullite: a substituted alumina. Am Mineral 62: 747–755
Cesnokov B, Kotrly M, Nisanbaev T (1998) Abraumhalden und Aufschlüsse im Tscheljabinsker Kohlenbecken - ein reicher Mineralienkuchen. Mineral Welt 3: 54–63
Chesnokov BV (1995) High-temperature mineralization of calcium chloride–silicates in the dumps of Chelyabinsk coal basin. Dokl Russian Akad Sci 343: 94–95
Chesnokov BV (1997) New minerals from old-burning dumps of the Chelyabinsk coal basin (tenth report – a review of the results for 1982–1995 years). Ural Mineral Sbor 7: 5–32
Chesnokov BV (1999) An experience of technogenesis mineralogy – 15 years of investigation of burned spoil-heaps of coal mines, pits and concentrating mills of the Southern Urals. Ural Mineral Sbor 9: 138–167
Chesnokov BV, Tsherbakova EP (1991) The mineralogy of burned heaps in the Chelyabinsk coal basin. Nauka, Moscow, 152 pp
Chesnokov BV, Vilisov VA, Bazhenova LF, Bushmakin AF, Kotlyarov VA (1993) New minerals from old-burning dumps in Chelyabinsk (fifth report). Ural Mineral Sbor 2: 3–36
Cosca MA, Essene EJ, Geissman JW, Simmons WB, Coates DA (1989) Pyrometamorphic rocks associated with naturally burned coal beds, Powder River Basin, Wyoming. Am Mineral 74: 85–100
Deer WA, Howie RA, Zussman J (1982) Rock-forming minerals. Orthosilicates, vol 1A. Longman, London New York, 919 p
Dingwell DB (1989) Effect of fluorine on the viscosity of diopside liquid. Am Mineral 74: 333–338
Edgar AD, Pizzolato LA, Sheen J (1996) Fluorine in igneous rocks and minerals with emphasis on ultrapotassic mafic and ultramafic magmas and their mantle source regions. Mineral Mag 60: 243–257
Ekström TK (1972) The distribution of fluorine among some coexisting minerals. Contrib Mineral Petrol 34: 192–200
Foley SF, Taylor WR, Green DH (1986a) The effect of fluorine on phase relationships in the system $KAlSiO_4$–Mg_2SiO_4–SiO_2 at 28 kbar and the solution mechanism of fluorine in silicate melts. Contrib Mineral Petrol 93: 46–55
Foley SF, Taylor WR, Green DH (1986b) The role of fluorine and oxygen fugacity in the genesis of the ultrapotassic rocks. Contrib Mineral Petrol 94: 183–192
Grigoryeva LF, Makarova TA, Korytkova EN, Chigareva OG (1975) Synthetic amphibole asbestoses. Nauka, Leningrad, 250 p
Gualtieri A, Bellotto M, Artioli G, Clark SM (1995) Kinetic study of the kaolinite-mullite reaction sequence, part II. Mullite formation. Phys Chem Minerals 22: 215–222
Kleck WD, Foord EE (1999) The chemistry, mineralogy, and petrology of the George Ashley Block pegmatite body. Am Mineral 84: 695–707
Kogarko LN, Krigman LD (1981) Fluorine in silicate melts and magmas. Nauka, Moscow, 125 p
Kovalenko VI, Kovalenko NI (1976) Ongonites. Nauka, Moscow, 125 p
Lavrent'ev Yu G, Usova LV (1991) The program complex RMA-89 for quantitative X-ray microanalysis by Camebax Micro microprobe. J Analyt Chem 46: 67–75
Lepezin GG, Bul'bak TA, Sokol EV, Shvedenkov G Yu (1999) Fluid components in cordierites and their significance for metamorphic petrology. Russ Geol Geophys 40: 99–116
London D, Wolf MB, Morgan GB IV, Garrido MG (1999) Experimental silicate–phosphate equilibria in peraluminous granitic magmas, with a case study of the Albuquerque batholith at Izes Arroyos, Badajos, Spain. J Petrol 40: 215–240
Lotova EV, Nigmatulina EN (1989) Genetic peculiarities of cordierites from fused rocks. Soviet Geol Geophys 30: 65–71

Luth RW (1988a) Raman spectroscopic study of the solubility mechanisms of F in glasses in the system $CaO–CaF_2–SiO_2$. Am Mineral 73: 297–305

Luth RW (1988b) Effects of phase equilibria and liquid structure in the system $NaAlSiO_4–CaMgSi_2O_6–SiO_2$. Am Mineral 73: 306–312

Nash WP (1993) Fluorine iron biotite from the Honeycomb Hills rhyolite, Utah: the halogen record of decompression in a silicic magma. Am Mineral 78: 1031–1040

Pesquera A, Torres-Ruiz J, Gil-Crespo PP, Velilla N (1999) Chemistry and genetic implications of tourmaline and Li–F–Cs micas from the Valdeflores area (Cáceres, Spain). Am Mineral 84: 55–69

Pouchou JL, Pichoir F (1985) 'PAP' ($\varphi\varphi\rho\rho z$) procedure for improved quantitative microanalysis. In: *Armstrong JT* (ed) Microbeam analysis. San Francisco Press, San Francisco, pp 104–106

Putilin Yu M, Belykova Yu A, Golenko VP (1987) Synthesis of minerals, part 2. Nedra, Moscow, 256 p

Putilin Yu M, Golenko VP, Yarotskaya EG, Andreev ME, Polyansky EV, Yarotsky VG (1992) Pyrogenic synthesis of silicates: reference book. Nedra, Moscow, 224 p

Sharygin VV, Sokol EV, Nigmatulina EN, Lepezin GG, Kalugin VM, Frenkel AE (1999) Mineralogy and petrography of technogenous parabasalts in the Chelyabinsk coal basin. Russ Geol Geophys 40: 879–889

Schreyer W, Maresch WV, Daniels P, Wolfsdorff P (1990) Potassic cordierites: characteristic minerals for high-temperature, very low-pressure environments. Contrib Mineral Petrol 105: 162–172

Stoppa F, Sharygin VV, Cundari A (1996) New mineral data from kamafugite–carbonatite association: the melilitolite from Pian di Celle, Italy. Mineral Petrol 61: 27–45

Sokol E, Volkova N, Lepezin G (1998) Mineralogy of pyrometamophic rocks associated with naturally burned coal-bearing spoil-heaps of the Chelyabinsk coal basin, Russia. Eur J Mineral 10: 1003–1014

Sokol EV, Kalugin VM, Sharygin VV, Nigmatulina EN (2000) Genesis of ferriferrous paralavas in the Chelyabinsk lignite basin. Ural Geol 6: 159–164

Takusagawa N, Saito H (1972) Relation between microstructure and mechanical strength of crystallized glasses having the chemical composition of fluor-richterite, containing Al. J Ceram Soc Jpn 80: 365–374

Authors' address: *E. V. Sokol, E. N. Nigmatulina,* and *N. I. Volkova,* United Institute of Geology, Geophysics and Mineralogy of Russian Academy of Sciences, Koptyug pr., 3, Novosibirsk, 630090, Russia, e-mail: sokol@uiggm.nsc.ru; nvolkova@uiggm.nsc.ru